catalysts

MDPI

Article

$TiCl_4/MgCl_2$/MCM-41 Bi-Supported Ziegler–Natta Catalyst: Effects of Catalyst Composition on Ethylene/1-Hexene Copolymerization

Xiaoyu Liu [1,†], Wenqi Guo [1,†], Xueer Wang [1], Yintian Guo [2,3], Biao Zhang [4], Zhisheng Fu [1], Qi Wang [1] and Zhiqiang Fan [1,*]

[1] MOE Key Laboratory of Macromolecular Synthesis and Functionalization, Department of Polymer Science and Engineering, Zhejiang University, Hangzhou 310027, China; xiaoyu_liu@zju.edu.cn (X.L.); guowq@zju.edu.cn (W.G.); wang_xe@zju.edu.cn (X.W.); fuzs@zju.edu.cn (Z.F.); wangq@zju.edu.cn (Q.W.)
[2] Zhejiang Hetian Chemical Co., Ltd., Hangzhou 310023, China; guoyintian@sinochem.com
[3] Sinochem Lantian Zhejiang Research Institute of Chemical Industry Co., Ltd., Hangzhou 310023, China
[4] Zhejiang Sinopont Technology Co., Ltd., Xiaoshan, Hangzhou 311254, China; zhangbiao@sinopont.com
* Correspondence: fanzq@zju.edu.cn
† These authors contributed equally to this work.

Abstract: $TiCl_4/MgCl_2$/MCM-41 type bi-supported Ziegler-Natta catalysts with different $MgCl_2$/MCM-41 ratios were synthesized by adsorbing $TiCl_4$ onto $MgCl_2$ crystallites anchored in mesopores of MCM-41 (mesoporous silica with 3.4 nm pore size). Ethylene/1-hexene copolymerization with the catalysts was conducted at different 1-hexene concentrations and ethylene pressures. $MgCl_2$/MCM-41 composite supports and the catalysts were characterized by X-ray diffraction (XRD), nitrogen adsorption analysis (BET), and elemental analysis. The copolymers were fractionated by extraction with boiling *n*-heptane, and comonomer contents of the fractions were determined. Under 4 bar ethylene pressure, the bi-supported catalysts showed higher activity and a stronger comonomer activation effect than the $TiCl_4/MgCl_2$ catalyst. In comparison with the $TiCl_4/MgCl_2$ catalyst, the bi-supported catalysts produced much less copolymer fraction of low molecular weight and high 1-hexene content, meaning that the active center distribution of the catalyst was significantly changed by introducing MCM-41 in the support. The copolymer produced by the bi-supported catalysts showed similar melting temperature to that produced by $TiCl_4/MgCl_2$ under the same polymerization conditions. The space confinement effect of the mesopores of MCM-41 on the size and structure of $MgCl_2$ crystallites is proposed as the main reason for the special active center distribution of the bi-supported catalysts.

Keywords: Ziegler-Natta catalyst; bi-supported; ethylene/1-hexene copolymerization; MCM-41; $MgCl_2$

Citation: Liu, X.; Guo, W.; Wang, X.; Guo, Y.; Zhang, B.; Fu, Z.; Wang, Q.; Fan, Z. $TiCl_4/MgCl_2$/MCM-41 Bi-Supported Ziegler–Natta Catalyst: Effects of Catalyst Composition on Ethylene/1-Hexene Copolymerization. *Catalysts* **2021**, *11*, 1535. https://doi.org/10.3390/catal11121535

Academic Editor: Abel Santos

Received: 17 November 2021
Accepted: 13 December 2021
Published: 16 December 2021

1. Introduction

Polyethylene (PE) is a general-purpose synthetic resin with the largest production volume (about 100 million tons per annal) among synthetic polymers. Among the three major PE categories (low density polyethylene, high density polyethylene, linear low density polyethylene), high density polyethylene (HDPE) and linear low density polyethylene (LLDPE) are produced by the catalytic copolymerization of ethylene with C_4~C_8 α-olefins. $TiCl_4/MgCl_2$ (single support) and $TiCl_4/MgCl_2/SiO_2$ (bi-support) type heterogeneous Ziegler–Natta (Z-N) catalysts play major roles in the production of HDPE and LLDPE [1,2]. Though these Z–N catalysts show excellent performance in large-scale industrial production for their high activity and satisfactory control over the polymer particle morphology, their PE products have rather broad chemical composition distribution (CCD) because of the presence of multiple active sites [3–5]. Because the α-olefin comonomer is highly enriched in fractions of low molecular mass [4–6], HDPE and LLDPE produced with Z-N catalysts show poorer mechanical properties than PE produced with single-site catalysts like metallocenes [7–9]. It is seen that the broad CCD of Z–N based PE resins needs to

be improved. In the past two decades, many efforts have been devoted to improving the ethylene–α-olefin copolymerization performance of Z-N catalysts [10–17]. However, improvements in ethylene copolymer's CCD were not satisfactory in many of these efforts.

In the last decades, mesoporous inorganic materials (e.g., MCM-41, SBA-15, AAO) with uniform pore size and very large surface area were used as a support of metallocene or other organometallic catalysts and tested for catalytic ethylene polymerization [18–26] and ethylene-α-olefin copolymerization [26–35]. In comparison with homogeneous catalysts, metallocene catalysts immobilized on mesoporous supports show a serious of unique performances, like producing PE with nanofibrous morphology [18,21] and special mechanical properties [20,25]. The space confinement effects of mesoporous support on the active sites were considered as the main reason for the unique performances. Similar concept has been extended to developing $MgCl_2$-supported Z-N catalysts. Semsarzadeh et al. [36] prepared two kinds of bi-supported Z-N catalysts, $TiCl_4/MgCl_2$/MCM-41 and $TiCl_4/MgCl_2/SiO_2$, and found that the catalyst containing MCM-41 showed higher activity than the one with SiO_2 in catalyzing ethylene polymerization. Similar ethylene polymerization behaviors of bi-supported catalysts containing a mesoporous support are reported by other researchers [37–40]. To the best of our knowledge, ethylene-α-olefin copolymerization with $TiCl_4/MgCl_2$/MCM-41 type bi-supported Z-N catalysts has not been reported in open-published journals.

In the literature on ethylene-α-olefin copolymerization with metallocene immobilized on mesoporous supports, strong effects of support pore size on the copolymerization activity, α-olefin incorporation rate, and copolymer's CCD were reported [28–34]. Large-pored catalysts were found to exhibit higher 1-hexene incorporation rates [29]. However, the effects of mesoporous support on ethylene-α-olefin copolymerization with $TiCl_4/MgCl_2$/MCM-41 type bi-supported Z-N catalysts are still unclear. In this work, MCM-4/$MgCl_2$ bi-supported Z-N catalysts with different MCM-4/$MgCl_2$ mass ratios were prepared by adsorbing $TiCl_4$ onto $MgCl_2$ crystallites that are anchored in nanochannels of MCM-41. These catalysts were used for catalyzing ethylene-1-hexene copolymerization under different ethylene pressure and ethylene/1-hexene feed ratios. Significant effects of the MCM-41 support on the catalytic activities and chain structure of the ethylene-1-hexene copolymers were observed, which are beneficial to the polymer performances.

2. Results and Discussions

2.1. Characterization of Supports and Catalysts

Five supported Ziegler-Natta catalysts were respectively prepared by anchoring $TiCl_4$ on activated $MgCl_2$, MCM-41 and $MgCl_2$/MCM-41 composite supports with different composition. According to literature reports, impregnating $MgCl_2$ in mesoporous silica like MCM-41 lead to anchoring of $MgCl_2$ crystallites in nanopores of the silica, owing to strong interaction of $MgCl_2$ with hydroxyl groups on inner walls of MCM-41 [38,41,42]. The MCM-41 mesoporous silica used to prepare the composite supports was calcinated at 500 °C to remove most of its hydroxyl groups on the outer surface. This can ensure that most $MgCl_2$ in $MgCl_2$/MCM-41 support is anchored in nanopores of MCM-41.

XRD analysis of the activated $MgCl_2$ precipitated from THF solution and the $MgCl_2$/MCM-41 bi-supports were first made and compared with XRD pattern of commercial anhydrous $MgCl_2$ (see Figure 1). The commercial $MgCl_2$ with α-phase and small surface area showed a strong peak at $2\theta = 15°$, which corresponds to the periodical stacking of Cl-Mg-Cl triple-layers, but this peak was absent in the activated $MgCl_2$ and $MgCl_2$/MCM-41 supports. The appearance of broad asymmetric peaks at $2\theta = 35°$ and $2\theta \approx 50°$ in XRD of the activated $MgCl_2$ and $MgCl_2$/MCM-41 indicated that both of them contain δ-phase $MgCl_2$ with small crystal size [43]. In the XRD pattern of $MgCl_2$/MCM-41, the peaks appearing at $2\theta = 3\sim6$ in the XRD of pure MCM-41 were not observed, possibly attributable to the filling of $MgCl_2$ in the meso-pores of MCM-41 (XRD pattern of calcinated MCM-41 can be seen in Figure S1).

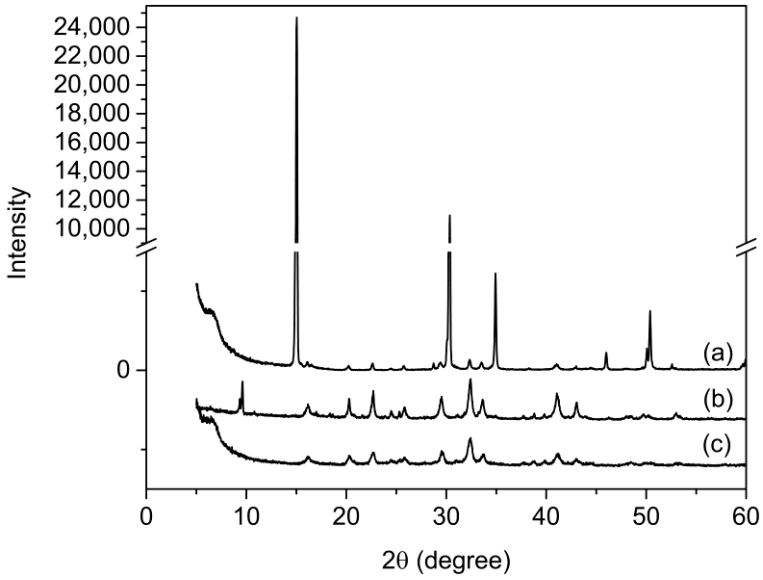

Figure 1. XRD patterns of (**a**) α-phase anhydrous $MgCl_2$, (**b**) activated $MgCl_2$ and (**c**) MCM-41/$MgCl_2$ (MM4).

The solid-phase structure of the supports was analyzed by N_2 volumetric measurement. As shown in Table 1, the $MgCl_2$/MCM-41 supports had a specific surface area and pore volume larger than the activated $MgCl_2$, but lower than the calcinated MCM-41. This phenomenon can be explained by the partial blocking of mesopores of MCM-41 by $MgCl_2$ in the composite support, since the large specific surface area of MCM-41 is mainly attributed to its mesopores. The $MgCl_2$/MCM-41 support with higher $MgCl_2$ load (sample MM4) had a smaller specific surface area than that with a lower $MgCl_2$ load (sample MM5), meaning that the mesopores of MCM-41 could be filled by $MgCl_2$ in the composite supports.

Table 1. Specific surface area and pore parameters of supports [a].

Support	Specific Surface Area (m^2/g)	Pore Volume (cm^3/g)	Average Pore Radius (nm)
$MgCl_2$	159.6	0.66	3.8
MCM-41	1021.7	1.02	2.7
MM4	606.1	0.88	2.7
MM5	697.7	0.88	3.1

[a] Determined by BET method; MM4 and MM5 are $MgCl_2$/MCM-41 composite with m($MgCl_2$)/m(MCM-41) (mass ratio) of $\frac{1}{2}$ and 1/3, respectively.

Five supported catalysts were prepared by anchoring $TiCl_4$ on activated $MgCl_2$, pure MCM-41, and three $MgCl_2$/MCM-41 composites, respectively. Ti and Mg contents of these catalysts were determined, and the results are listed in Table 2, which shows that Ti content of the $TiCl_4$/MCM-41 catalyst (cat-2) was even higher that of the $TiCl_4$/$MgCl_2$ catalyst (cat-1), possibly owing to the much larger specific surface area of MCM-41 than the activated $MgCl_2$. $TiCl_4$ could react with hydroxyl groups inside the mesopores of MCM-41 to form -SiO-$TiCl_3$ type anchored Ti species [38]. With the decrease of $MgCl_2$/MCM-41 mass ratio of the support from 1/1 (cat-3) to 1/2 (cat-4) and 1/3 (cat-5), the Mg/Ti molar ratio of the corresponding catalyst also markedly decreased. It seems that when $MgCl_2$ occupies the internal surface of the mesopores in MCM-41, less $TiCl_4$ can be anchored on MCM-41 to form $-SiO-TiCl_3$ type species. The Mg/Ti molar ratio of cat-3 that has the highest $MgCl_2$/MCM-41 ratio was close to that of cat-1, which contains no MCM-41, meaning that most of the $TiCl_4$ in cat-3 is anchored on $MgCl_2$ crystallites. In cat-4 and cat-5 that have lower $MgCl_2$ contents, a significant part of $TiCl_4$ could be directly anchored on the surface of MCM-41.

Table 2. Chemical composition of catalysts [a].

Catalyst	Cat-1	Cat-2	Cat-3	Cat-4	Cat-5
Ti, wt%	5.20	6.00	3.63	5.85	4.84
Mg, wt%	13.20	0	7.49	6.98	4.95
n(Mg)/n(Ti) [b]	5.0	0	4.1	2.4	2.0
m($MgCl_2$)/m(MCM-41) [c]	1/0	0/1	1/1	1/2	1/3

[a] Ti content was determined by UV-vis analysis, Mg content was determined by ICP analysis. [b] Mg/Ti molar ratio of the catalyst. [c] Mass ratio of $MgCl_2$ to MCM-41 of the catalyst support.

2.2. Polymerization Activity

The polymerization of ethylene and copolymerization of ethylene/1-hexene with the prepared catalysts were conducted under 1 bar and 4 bar ethylene pressure, respectively. For (co)polymerization under 1 bar, the activity of cat-2 ($TiCl_4$/MCM-41 mono-supported catalyst) was only 2~10% of that of cat-1 ($TiCl_4$/$MgCl_2$ mono-supported catalyst, see Table 3). Similar phenomena have been reported in literatures dealing with similar catalysts [36,37]. It means that $MgCl_2$ plays an essential role in enhancing polymerization activity of supported Z-N catalyst [44]. The catalysts containing $MgCl_2$ (cat-1, cat-3, cat-4, and cat-5) showed similar activity at 1 bar ethylene pressure, and the activity evidently increased with increase of 1-hexene concentration. Under 4 bar ethylene pressure, the ethylene/1-hexene copolymerization activity was about 10 times higher than that conducted under 1 bar, while the activity of the $MgCl_2$/MCM-41 bi-supported catalysts became higher than that of the $MgCl_2$-supported catalyst (see Figure 2 and Table 3). It is interesting that the activity of the bi-supported catalysts increased with decrease of $MgCl_2$/MCM-41 ratio (the only exception was the higher activity of cat-4 than cat-5 at [H] = 0.6 mol/L). Explanations on this phenomenon will be given after analyzing chemical structure and particle morphology of the polymerization products.

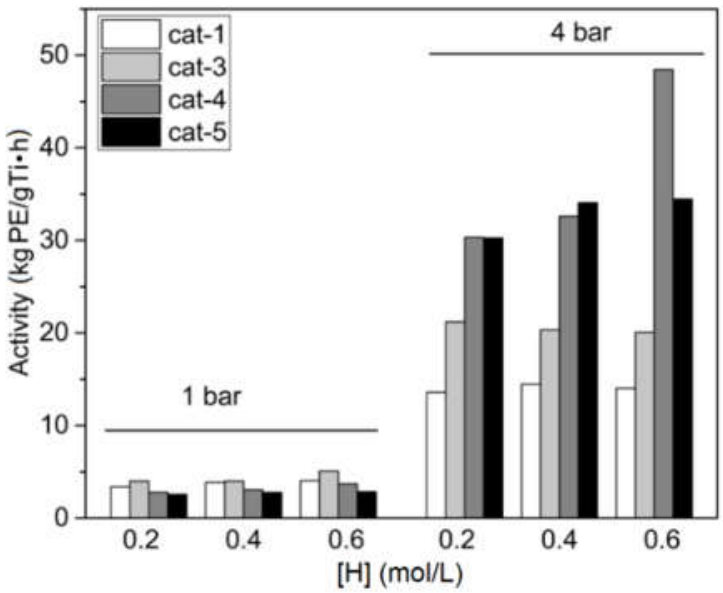

Figure 2. Copolymerization activities of cat-1, cat-3, cat-4 and cat-5 under 1 bar and 4 bar ethylene pressure.

Table 3. Results of ethylene/1-hexene copolymerization with different Ziegler-Natta catalysts under different ethylene pressure [a].

Entry	Catalyst	Pressure (Bar)	[H] (mol/L)	Activity (kgPE/(gTi·h))	M_w [c] (kg/mol)	$Đ$ [c]	T_m [d] (°C)	ΔH_m [d] (J/g)
1	cat-1	1	0	1.47	495	8.7	133	168.4
2	cat-1	1	0.2	3.37	255	23.8	124	94.5
3	cat-1	1	0.4	3.86	208	21.0	123	58.4
4	cat-1	1	0.6	4.04	156	17.7	123	42.5
5	cat-2	1	0	0.15	–	–	133	112.5
6	cat-2	1	0.2	0.12	–	–	130	84.5
7	cat-2	1	0.4	0.10	–	–	129	70.5
8	cat-2	1	0.6	0.09	–	–	129	70.1
9	cat-3	1	0	2.39	393	9.8	134	172.7
10	cat-3	1	0.2	3.99	167	15.2	125	97.1
11	cat-3	1	0.4	3.99	166	24.1	124	52.1
12	cat-3	1	0.6	5.07	138	18.7	123	41.4
13	cat-4	1	0	1.26	455	10.5	134	173.4
14	cat-4	1	0.2	2.79	231	23.1	124	99.7
15	cat-4	1	0.4	3.06	184	18.6	124	55.6
16	cat-4	1	0.6	3.70	130	17.1	123	39.1
17	cat-5	1	0	1.17	569	9.3	133	167.5
18	cat-5	1	0.2	2.55	291	23.5	124	100.5
19	cat-5	1	0.4	2.77	173	22.5	123	62.8
20	cat-5	1	0.6	2.85	195	19.9	123	43.0
21 [b]	cat-1	4	0.2	13.58	414	5.5	127	131.4
22	cat-1	4	0.4	14.47	287	8.9	124	114.6
23	cat-1	4	0.6	14.01	239	10.0	123	97.2
24	cat-3	4	0.2	21.18	362	8.2	127	132.5
25	cat-3	4	0.4	20.33	295	10.7	124	117.0
26	cat-3	4	0.6	20.07	274	9.1	123	98.0
27	cat-4	4	0.2	30.34	405	7.4	129	129.8
28	cat-4	4	0.4	32.60	372	11.1	126	116.0
29	cat-4	4	0.6	48.43	310	8.9	124	113.4
30	cat-5	4	0.2	30.27	389	6.5	128	130.8
31	cat-5	4	0.4	34.07	417	7.9	127	120.9
32	cat-5	4	0.6	34.47	399	7.3	125	111.4

[a] Polymerization conditions: [Ti] = 6×10^{-4} mol/L; cocatalyst: $Al(C_2H_5)_3$; n(Al)/n(Ti) = 100; polymerization temperature: 60 °C; time = 30 min; *n*-heptane as solvent, [H] = initial 1-hexene concentration; [b] For polymerization runs under 4 bar ethylene pressure, [Ti] was reduced to 2×10^{-4} mol/L; [c] Weight-average molecular weight (M_w) and polydispersity index ($Đ$) determined by GPC; [d] Melting temperature (T_m) and melting enthalpy (ΔH_m) of polymer determined by DSC.

2.3. Polymer Structure

All copolymer samples produced by cat-1, cat-3, cat-4, and cat-5 were extracted by boiling *n*-heptane to fractionate each of them into two parts: boiling *n*-heptane soluble fraction (C7-s) and insoluble fraction (C7-in). Each fraction was analyzed by FT-IR to determine its 1-hexene content, and the results are listed in Tables 4 and S1. As a general trend, the C7-s content of the copolymer increased with increase of 1-hexene concentration ([H]) under both 1 bar and 4 bar ethylene pressure (see Figure 3 and Table S1), similar to the phenomena observed in our previous studies [4,14,17]. C7-s of copolymer produced under 1 bar was higher than that formed under 4 bar at the same [H], since ethylene concentration was higher under higher pressure. For both the copolymerization runs, under 1 bar and 4 bar, C7-s content of copolymer catalyzed by the three bi-supported catalysts was lower than the $MgCl_2$-supported catalyst (the blank catalyst without MCM-41). The difference became more evident when the copolymers were produced under 4 bar. When cat-5 with the highest MCM-41 load was used as catalyst, the C7-s content of its copolymer formed at

[H] = 0.6 mol/L and 4 bar was only about 30% of the copolymer produced by cat-1 under the same conditions. In contrast, copolymers produced by cat-2 that has a much lower MCM-41 load contained a similar amount of C7-s fraction to those of cat-1.

Table 4. Boiling *n*-heptane extraction results of copolymer catalyzed by cat-1, cat-3, cat-4 and cat-5 under 4 bar.

Entry	Catalyst	[H] (mol/L)	C_6 [a] (mol%)	Conversion (%) [b]	C7-s		C7-in	
					Fraction (wt%)	C_6 [a] (mol%)	Fraction (wt%)	C_6 [a] (mol%)
21	cat-1	0.2	2.4	27.6	1.1	-	98.9	2.4
22	cat-1	0.4	2.1	13.3	10.0	6.9	90.0	1.6
23	cat-1	0.6	3.6	14.7	27.1	8.2	72.9	2.1
24	cat-3	0.2	0.9	16.6	3.5	-	96.5	0.9
25	cat-3	0.4	2.7	23.7	13.8	8.1	86.2	1.9
26	cat-3	0.6	3.3	19.4	26.4	7.5	73.6	1.9
27	cat-4	0.2	1.1	28.9	3.2	-	96.8	1.1
28	cat-4	0.4	2.4	34.0	10.5	10.0	89.5	1.6
29	cat-4	0.6	3.2	45.4	14.5	9.5	85.5	2.3
30	cat-5	0.2	1.1	28.9	2.6	-	97.4	1.1
31	cat-5	0.4	2.0	29.8	7.1	8.8	92.9	1.5
32	cat-5	0.6	2.4	24.6	8.3	9.0	91.7	1.8

[a] 1-Hexene content of the whole copolymer determined by FTIR. [b] Conversion rate of 1-hexene.

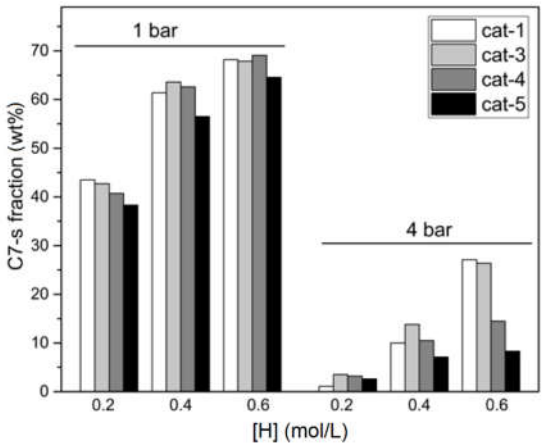

Figure 3. Change C7-s fraction weight of ethylene/1-hexene copolymer with initial 1-hexene concentration.

The 1-Hexene contents of the original copolymer samples and their fractions were determined, and the results are shown in Figures 4 and S2. It can be seen that the hexene content of the copolymer produced under 1 bar was slightly enhanced by introducing MCM-41 in the support, but less 1-hexene was incorporated in the copolymer produced under 4 bar when MCM-41 was introduced. The 1-Hexene contents of the C7-in fraction were hardly changed by MCM-41, but the 1-hexene content of the C7-s fraction slightly increased with increase of MCM-41 in the catalyst.

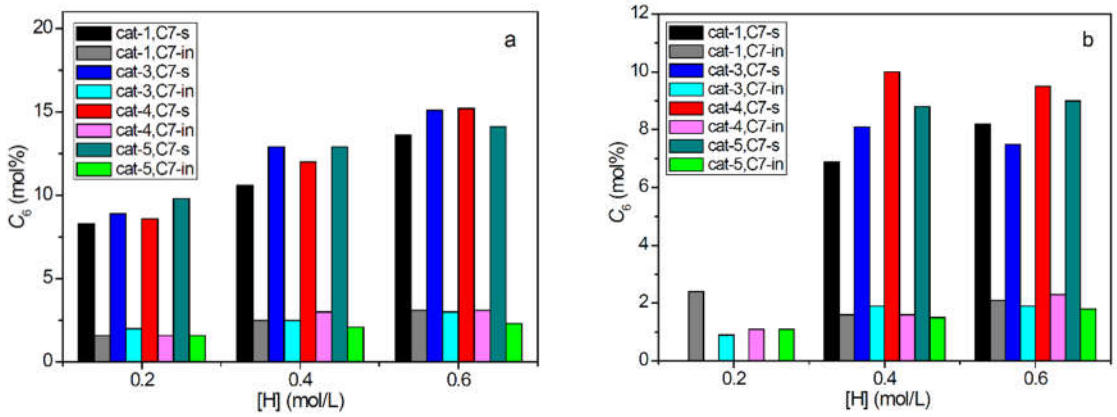

(**a**) (**b**)

Figure 4. 1-Hexene content of copolymer fractions produced under 1 bar (**a**) and 4 bar (**b**).

Thermal analysis of the copolymer samples and their fractions was performed, which provided information regarding crystalline phases indirectly reflecting the chain structure of the copolymer. As shown in Tabels 3, 5 and S2, the melting temperature and melting enthalpy of the copolymer tended to decrease with increase of 1-hexene concentration, since the incorporated 1-hexene units can interrupt the crystallization of polyethylene segments, leading to smaller crystalline phases and thinner crystalline lamellae. Introducing MCM-41 in the catalyst hardly influenced melting temperature, but the melting enthalpy of C7-s part decreased with a decreasing $MgCl_2$/MCM-41 ratio. This can be largely attributed to the higher 1-hexene content of C7-s part formed by the bi-supported catalysts, especially for C7-s formed under 4 bar. For the C7-in fractions, their melting enthalpy was only slightly influenced by the introduction of MCM-41. It seems that the active centers producing this part of the copolymer have the same catalytic features in both $TiCl_4/MgCl_2$ and $TiCl_4/MgCl_2$/MCM-41 catalysts.

Table 5. Thermal properties of copolymers and their fractions catalyzed by cat-1, cat-3, cat-4 and cat-5 under 4 bar.

Entry	Catalyst	[H] (mol/L)	C7-s		C7-in	
			T_m (°C)	ΔH_m (J/g)	T_m (°C)	ΔH_m (J/g)
21	cat-1	0.2	114	104.3	127	132
22	cat-1	0.4	119	60.5	124	123
23	cat-1	0.6	116	53.0	123	115
24	cat-3	0.2	117	73.8	127	137
25	cat-3	0.4	118	59.3	124	125
26	cat-3	0.6	118	50.1	123	112
27	cat-4	0.2	117	54.5	129	134
28	cat-4	0.4	116	41.3	125	125
29	cat-4	0.6	117	41.3	124	120
30	cat-5	0.2	116	41.7	128	124
31	cat-5	0.4	117	42.3	124	126
32	cat-5	0.6	117	46.1	125	120

As shown in Table 3, copolymers produced by bi-supported catalysts under 4 bar had higher M_w than that produced by the blank catalyst when [H] was larger than 0.2 mol/L. This can be explained by the lower C7-s content of the former (see Figure 3). It is well documented that the C7-s fraction of the ethylene-1-hexene copolymer synthesized by Z-N catalysts has a much lower molecular weight than the C7-in fraction [4,14,17]. Therefore,

variation of C7-s content in copolymer will lead to evident changes in its average molecular weight and molecular weight distribution. Because the copolymers produced by different catalysts under 1 bar had similar C7-s contents, their M_w values varied in a narrower range.

Comonomer content and molecular weight of the (co)polymers produced by cat-2 ($TiCl_4$/MCM-41 catalyst) were not determined due to a lack of sufficient samples. DSC analysis on these copolymers showed that they had higher melting temperature and melting enthalpy in comparison with those produced by the catalysts containing $MgCl_2$, meaning that cat-2 had poorer ability of incorporating 1-hexene in the polymer chains.

Summarizing the results of chain structure characterization on the copolymers produced by cat-1, cat-3, cat-4, and cat-5, it is clear that these polymers have similar structural features in terms of 1-hexene content, crystalline structure, and molecular weight. The main differences between the polymers of blank Z-N catalyst and those of the bi-supported Z-N catalysts are evidenced by the lower C7-s content of the latter when ethylene concentration was relatively high. These kinds of change in copolymer structure are beneficial to its application properties. In ethylene-α-olefin copolymers, the α-olefin comonomer like 1-hexene is introduced in the polymer chain in order to reduce the crystallinity and lamellae thickness. This kind of polymer shows lower melting temperature, lower stiffness, improved impact strength, and improved optical transparency in comparison with ethylene homopolymer, making the former more suited for applications like polymer films and soft/tough plastics. In such a polymer, the part of copolymer with high α-olefin content and low molecular weight hardly contributes to the material's mechanical properties, but may damage the film performance for its solubility in organic solvents at room temperature. When we compare sample 23 produced by cat-1 and sample 34 produced by cat-5, their melting temperatures are all 10~15 °C lower than that of the ethylene homopolymer (T_m = 137~140 °C), meaning that they are all suited for application as plastic film. However, the C7-s content of sample 23 was nearly three times higher than that of sample 34. Such a large amount of soft and weak (for low M_w of the C7-s fraction) components in sample 23 will lead to lower mechanical strength and poorer solvent resistance of its film product as compared with sample 34. Therefore, the bi-supported catalysts, especially those with relatively low $MgCl_2$/MCM-41 ratio, can produce copolymer with better properties than the conventional $TiCl_4/MgCl_2$ type Z-N catalyst.

2.4. Morphology of Nascent Polymer Particles

The morphology of polyethylene particles produced by the $TiCl_4$/MCM-41 catalyst (cat-2) is shown in Figure 5. The PE particles were loose aggregates of micrometer-sized short rods. Such morphology can be attributed to the replication of the rod-like MCM-41 particles in the polymerization process. A few nano-fibrils can be seen on parts of the short rods, which should be caused by extrusion of PE chains from mesopores of the support [22,23,36,40]. However, the nano-fibrils on PE formed by cat-2 were much shorter, and their space density was much lower than that of MCM-41 supported catalysts reported in the literature, since cat-2 has much lower catalytic activity than those producing high-yield nano-fibrils (the sample of Figure 5 has a polymer/catalyst mass ratio of only 4.5). When most of the active sites are anchored on the internal surface of the nano-pores of MCM-41, a low polymer growth rate over large active surfaces will lead to a slow rate of PE extrusion from the mesopores, and more difficult formation of nano-fibrils. The good replication of support morphology in PE/cat-2 particles implies that most of $TiCl_4$ in cat-2 are anchored inside the meso-pores of MCM-41.

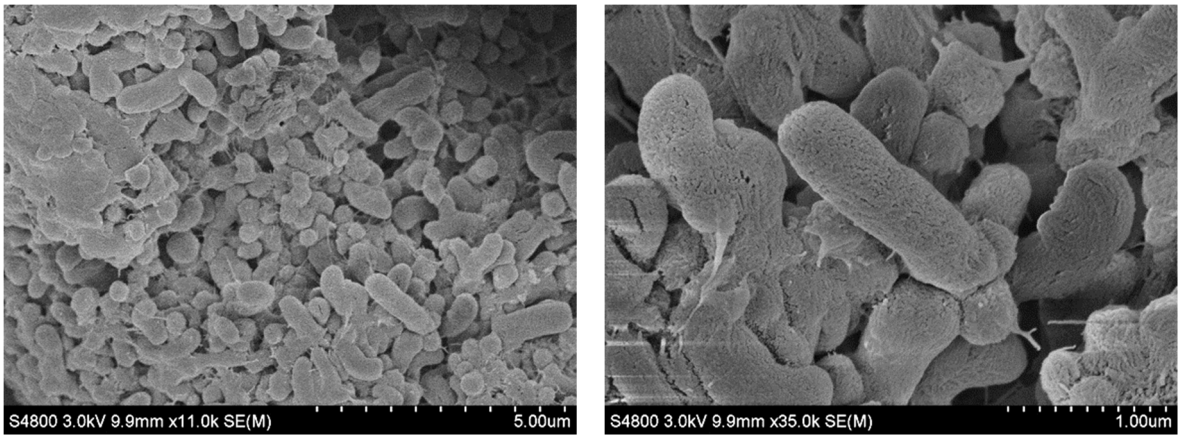

(**a**) (**b**)

Figure 5. SEM pictures of nascent polyethylene particles catalyzed by cat-2 under 1 bar, (**a**) Magnification ×11 k; (**b**) Magnification ×35 k.

Typical morphologies of PE particles produced by the bi-supported catalysts under 1 bar ethylene pressure are shown in Figure 6. In contrast to the replication phenomenon in PE/cat-2 particles, the morphology of regular short rods of MCM-41 was seriously distorted in these particles. In the PE/cat-3 particles, irregular sub-particles of 0.2~1 μm can be seen, which were tightly connected with each other. In the PE/cat-5 particles, sub-particles were hardly distinguishable, as they were strongly merged in micrometer-sized particles.

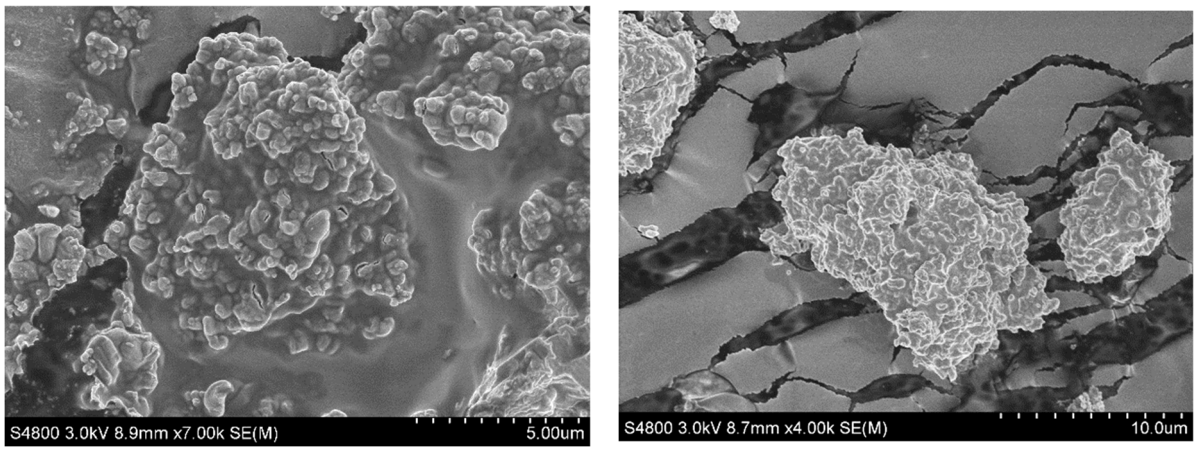

(**a**) (**b**)

Figure 6. Morphology of nascent polyethylene particles produced under 1 bar with (**a**) cat-3 and (**b**) cat-5.

Morphologies of nascent copolymer particles produced by the bi-supported catalysts under 4 bar were significantly different from those of PE produced under 1 bar. Unlike the compact particles produced by bi-supported catalysts under 1 bar, the particles formed at 4 bar were very loose aggregates of irregular sub-particles, many of them being covered by randomly distributed thread-like structures (see Figures 7 and S5). This kind of morphology is also present in nascent copolymer particles produced by cat-1 (the mono-supported Z-N catalyst, see Figure S6). It should be noted that the fiber-like and thread-like structures in Figure 7 are clearly different from the long and thin PE nano-fibers reported in the literature, produced with similar $MgCl_2$/MCM-41 bi-supported catalysts [40]. This means that no PE nano-fibers were formed by the bi-supported catalysts studied in this work. In the literature, the PE nano-fibers formed by MCM-41 supported catalysts are explained as the result of extrusion polymerization, in which the mesopores of MCM-41 confine the movement of

PE chains formed on active centers anchored inside the mesopores [22,23,36,40]. However, the nano-sized channels of MCM-41 could be broken up when the rate of polymer growth inside the channels exceeds a certain threshold level, as the pressure exerted on the walls of channels by the growing polymer will increase with the polymerization rate. This could be the main reason for the absence of nano-fibers in PE produced by bi-supported catalysts under 4 bar. In other words, the mesopores of bi-supported catalysts may be largely broken up during ethylene-1-hexene copolymerization under 4 bar. The space confinement effects on active centers anchored in the mesopores will thus disappear, and the barriers to monomer diffusion from the reaction medium to the active centers will be reduced. As a result, the polymerization rate will be evidently enhanced. This mechanistic model can be used to explain the much larger extent of polymerization rate enhancement of the bi-supported catalysts than the $MgCl_2$-supported catalyst when ethylene pressure was raised from 1 to 4 bar (see Figure 2). The absence of nano-fibers in PE produced with the bi-supported catalysts under 1 bar could be attributed to the low polymerization rate of such catalysts [36,40].

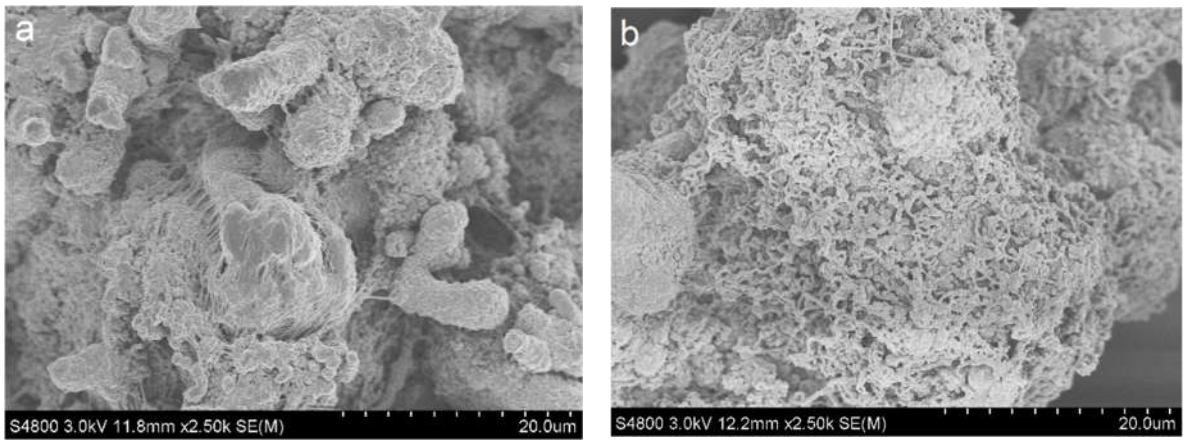

(**a**) (**b**)

Figure 7. Morphology of nascent copolymer particles synthesized under 4 bar ethylene pressure and [H] = 0.2 mol/L with (**a**) cat-4 and (**b**) cat-5.

The changes of catalytic activity and copolymer chain structure with decrease of $MgCl_2$/MCM-41 mass ratio can also be explained by the same mechanism. As seen in Figures 2 and 3, the differences between the bi-supported catalyst and the blank Z-N catalyst became more evident when $MgCl_2$/MCM-41 ratio decreased. This means that a larger percentage of $MgCl_2$ is adsorbed on locations outside the mesopores of MCM-41 in bi-supported catalyst with high $MgCl_2$/MCM-41 ratio (cat-3), making cat-3 behave like a mixture of traditional $MgCl_2$-supported catalyst and $MgCl_2$/MCM-41 bi-supported catalyst. The catalyst with the lowest $MgCl_2$/MCM-41 ratio (cat-5) exhibited the largest extent of differences from the blank Z-N catalyst, meaning that most of its $MgCl_2$ and thus $TiCl_4/MgCl_2$ species are located inside the mesopores of MCM-41.

The strong differences in catalytic features between the bi-supported catalyst and blank Z-N catalyst could be explained by space confinement effect in MCM-41 mesopores on structure of $MgCl_2$ crystallites. In traditional $MgCl_2$-supported Z-N catalysts, the average size of $MgCl_2$ crystallites varies between 3–13 nm, depending on the method of catalyst preparation [45–49]. In the bi-supported catalysts, the growth of $MgCl_2$ crystallites inside the mesopores with 3.4 nm pore size will be strongly limited, resulting in a relatively small crystallite size and narrower size distribution. It is expectable that a larger fraction of stereochemically open surface sites (e.g., corners) is present on smaller $MgCl_2$ crystallites. $TiCl_4$ adsorbed on such sites will be less congested. As proposed in our previous work, $TiCl_4$ located on open and less congested surface sites could form Ti(II) species that incorporate less α-olefin comonomer [50]. This could be the reason for the lower C7-s content of

ethylene-1-hexene copolymer produced by the bi-supported catalysts, especially cat-5, which has a higher percentage of active centers inside the mesopores of MCM-41.

3. Materials and Methods

3.1. Chemicals

MCM-41 (3.4 nm pore size, Nanjing Xianfeng Nanomaterials Co. Ltd, Nanjing, China.) was calcinated at 500 °C for 2 h before use. Tetrahydrofuran (THF) and *n*-heptane (Sinopharm Chemical Reagent Co. Ltd, Shanghai, China.) were purified by refluxing over sodium for 6 h and distilled before use. Triethylaluminum (TEA, Albemarle, NC, USA) was diluted with *n*-heptane to 2 mol/L before use. Titanium tetrachloride ($TiCl_4$, Adamas, Shanghai, China) and $MgCl_2$ (Alfa Aesar Co., Shanghai, China) were used as received. 1-Hexene (98%, J&K Scientific, Shanghai, China) was distilled over metallic sodium before use. Ethylene gas (polymerization grade, SINOPEC, Shanghai, China) used in the polymerizations was purified by passing through columns of 4 Å molecular sieves and PEE deoxygenate catalyst (Dalian Samat Chemicals, Dalian, China).

3.2. Preparation of $MgCl_2$ and $MgCl_2$/MCM-41 Support

Anhydrous $MgCl_2$ (2.5 g) was introduced into a round-bottom flask in a glove box, before 60 mL THF was successively introduced to the flask under nitrogen, and the flask was heated to 95 °C under stirring until $MgCl_2$ was completely dissolved in THF. Fine $MgCl_2$/THF adduct particles were precipitated when the solution was cooled to 60 °C, and then THF was removed by evacuating the flask for 2 h, and the solid $MgCl_2$ support was stored in a glove box. For preparing the $MgCl_2$/MCM-41 support, a clear $MgCl_2$/THF solution was first prepared in the same procedures, and the hot solution was transferred to another flask containing designed amount of MCM-41. The suspension was stirred at 95 °C for 2 h, the temperature was reduced to 60 °C under nitrogen atmosphere, then the suspension was kept still for 15 min to settle down the $MgCl_2$/MCM-41 support. The THF was removed by evacuating the flask for 2 h at 60 °C, and the dried support was stored in a glove box.

3.3. Preparation of Ziegler-Natta Catalysts

Supported Ziegler-Natta catalysts using $MgCl_2$, $MgCl_2$/MCM-41, and MCM-41 as the support were respectively prepared by anchoring $TiCl_4$ on the support in similar procedures adopted in our previous work [51]. The support was first dispersed in 40 mL *n*-heptane at 40 °C, a calculated amount of $TiCl_4$ (Ti/Mg = 10 mol/mol) was added into the slurry. It was stirred at 90 °C for 2 h under the protection of nitrogen, then the slurry was cooled to 60 °C, kept still to settle down the solid catalyst, and the solvent was removed using syringe. The catalyst was washed by *n*-heptane for three times (each time 15 mL) at 60 °C, then dried by vacuum, and stored at −10 °C inside a glove box.

3.4. Ethylene Polymerization and Ethylene/1-Hexene Copolymerization

Ethylene (co)polymerization was carried out in a 100 mL Schlenk flask equipped with a magnetic stirring bar. Firstly, the flask was dried by heating under vacuum and refilling with nitrogen for three times. Then, it was filled with ethylene at 1 bar. Designed amounts of *n*-heptane, TEA, and 1-hexene (for copolymerization) were successively introduced into the flask. Weighed solid catalyst was then added to start the polymerization at 60 °C. Gaseous ethylene at 1 bar was continuously supplied to the flask during the polymerization. After a designed time, the polymerization was terminated with 95/5 mixture of ethanol and concentrated HCl. The produced polyethylene or ethylene/1-hexene copolymer powder was repeatedly washed with ethanol and filtered, then dried at 60 °C under vacuum for 6 h.

Pressurized ethylene/1-hexene copolymerization was carried out in a 300 mL Büchi autoclave with mechanical stirrer. All procedures were the same as the polymerization runs under atmospheric pressure, while gaseous ethylene at 4 bar was continuously supplied to the autoclave during the copolymerization.

3.5. Polymer Fractionation

Each copolymer was fractionated into two parts by solvent extraction. About 1 g polymer was extracted with boiling *n*-heptane in a Soxhlet extractor for 12 h. The boiling *n*-heptane soluble fraction (C7-s) was recovered by concentrating the solution and precipitating the polymer with isopropanol. Both the C7-s fraction and the part insoluble in boiling *n*-heptane (C7-in) were vacuum dried at 50 °C overnight and weighed.

3.6. Characterization

Powder X-ray diffraction analysis of the support was made using an Ultima IV diffractometer. The scans were performed from diffraction angle 2θ = 5° to 60°. The step size was 0.2° and the time per step was 12 s. The sample was placed on a special holder and the holder was sealed with a thin Mylar film to prevent contact of the samples with air and moisture. Nitrogen adsorption measurement was performed on an AUTOSORB-1-C instrument. The surface area and pore-size distribution were calculated by using the Brunnauer—-Teller (BET) method. The Ti content of the catalyst was determined by the UV-Vis method. A known quantity of catalyst was dissolved in sulfuric acid and treated with hydrogen peroxide to form peroxo-titanium complex, which is a yellow solution. The content of Ti was calculated from the absorbance of the solution at 410 nm recorded by a UV-vis spectrophotometer. The content of Mg was measured by inductively coupled plasm spectrometry (ICP).

The average molecular weight and polydispersity index (*Đ*) of the polymer samples were measured by high temperature gel permeation chromatography (HT-GPC, Agilent PL-220) with three PL mixed B columns (500~107) at 150 °C in 1,2,4-trichlorobenzene. Polystyrene standards were used to make universal calibration of the experimental GPC curves. The content of 1-hexene in the copolymers as well as the copolymer fractions was measured by the FTIR method that was calibrated by ^{13}C NMR analysis [52]. Differential scanning calorimetry (DSC) measurements were carried out on a TA Q200 DSC calorimeter. About 3~5 mg of sample was sealed in an aluminum sample cell. The sample was first melted at 160 °C for 5 min to erase the thermal history, and then cooled to 40 °C at a cooling rate of 10 °C/min, followed by reheating to 160 °C at a scanning rate of 10 °C/min to record the melting behavior. Scanning electron microscope (SEM) analysis of the nascent polymer particles was conducted with a Hitachi S4800 field-emission SEM (Hitachi High-Technologies Corp., Tokyo, Japan). The micrographs were taken at 3-kV acceleration voltage. Before SEM observations, all the sample surfaces were sputtered with a thin layer of gold.

4. Conclusions

$TiCl_4/MgCl_2$/MCM-41 type bi-supported Z-N catalysts with different $MgCl_2$/MCM-41 ratio were prepared in order to control the active center distribution and tailor the chain structure of the olefin copolymer they produce. The pore volume and specific surface area of MCM-41 were significantly reduced after immobilizing $MgCl_2$ on the mesoporous silica. Ethylene-1-hexene copolymerization activity of the bi-supported catalysts was comparable to that of a $TiCl_4/MgCl_2$ type Z-N catalyst. Under 4 bar ethylene pressure, the bi-supported catalysts showed a stronger comonomer activation effect than the $TiCl_4/MgCl_2$ catalyst, rendering higher activity of the former at relatively high 1-hexene concentration. In comparison with the $TiCl_4/MgCl_2$ catalyst, the bi-supported catalysts produced much less copolymer fraction of low molecular weight and high 1-hexene content, meaning that active center distribution of the catalyst was significantly changed by introducing MCM-41 in the support. The extent of active center distribution variation was enhanced by increasing MCM-41 content in the bi-supported catalyst. Ethylene/1-hexene copolymers produced by the bi-supported catalysts under 4 bar had a narrower composition distribution and molecular weight distribution than that produced by the traditional $MgCl_2$-supported Z-N catalyst. The copolymer produced by the bi-supported catalysts had a lower content of boiling *n*-heptane soluble fraction than that produced by the $TiCl_4/MgCl_2$ catalyst, but

the former showed greater similarity T_m than the latter. This kind of ethylene copolymer, combining the features of low soluble fraction and low melting temperature, will show better performances for applications such as polymer film. The particle morphology of nascent copolymer produced by the bi-supported catalysts was similar to that produced by the traditional $MgCl_2$-supported Z-N catalyst. Combining low cost and robustness in the industrial process with better copolymer properties, this kind of bi-supported Z-N catalyst could find important applications in the polyolefin industry.

Supplementary Materials: The following are available online at https://www.mdpi.com/article/10.3390/catal11121535/s1, Figure S1. XRD curve of MCM-41. Figure S2. Pore size distribution of $MgCl_2$, MCM-41 and two composite supports. Figure S3. 1-Hexene content of ethylene/1-hexene copolymer produced under 1 bar and 4 bar. Figure S4. DSC traces of unfractionated (co)polymers. Figure S5. Morphology of nascent copolymer particles synthesized under 4 bar ethylene pressure and [H] = 0.2 mol/L with cat-4 and cat-5 and Figure S6 Morphology of nascent copolymer particles synthesized under 4 bar ethylene pressure and [H] = 0.2 mol/L with cat-1. Table S1. Boiling *n*-heptane extraction results of copolymer catalyzed by cat-1, cat-3, cat-4 and cat-5 under 1 bar. Table S2. Thermal properties of copolymer and C7-s fraction produced by cat-1, cat-3, cat-4 and cat-5 under 1 bar.

Author Contributions: Conceptualization, Z.F. (Zhiqiang Fan), Q.W. and Z.F. (Zhisheng Fu); methodology, W.G.; formal analysis, X.L., W.G., X.W., Y.G. and B.Z.; investigation, X.L. and W.G.; data curation, W.G.; writing—original draft preparation, W.G.; writing—review and editing, Z.F. (Zhiqiang Fan); visualization, X.L., W.G., X.W., Y.G. and B.Z.; data interpretation, supervision, Q.W. and Z.F. (Zhisheng Fu); funding acquisition, Z.F. (Zhiqiang Fan). All authors have read and agreed to the published version of the manuscript.

Funding: This research was funded by National Natural Science Foundation of China (grant number U1462114, 51773178).

Data Availability Statement: Data are contained within the article.

Conflicts of Interest: The authors declare no conflict of interest.

References

1. Mülhaupt, R. Catalytic Polymerization and Post Polymerization Catalysis Fifty Years After the Discovery of Ziegler's Catalysts. *Macromol. Chem. Phys.* **2003**, *204*, 289–327. [CrossRef]
2. Claverie, J.P.; Schaper, F. Ziegler-Natta Catalysis: 50 Years After the Nobel Prize. *MRS Bull.* **2013**, *38*, 213–218. [CrossRef]
3. Kakugo, M.; Miyatake, T.; Mizunuma, K. Chemical Composition Distribution of Ethylene-1-Hexene Copolymer Prepared with Titanium Trichloride-diethylaluminum Chloride Catalyst. *Macromolecules* **1991**, *24*, 1469–1472. [CrossRef]
4. Chen, Y.P.; Fan, Z.Q. Ethylene/1-hexene copolymerization with $TiCl_4/MgCl_2/AlCl_3$ catalyst in the presence of hydrogen. *Eur. Polym. J.* **2006**, *42*, 2441–2449. [CrossRef]
5. Zhang, L.T.; Fan, Z.Q.; Fu, Z.S. Dependence of the Distribution of Active Centers on Monomer in Supported Ziegler-Natta Catalysts. *Chin. J. Polym. Sci.* **2008**, *26*, 605–610. [CrossRef]
6. Tso, C.C.; DesLauriers, P.J. Comparison of Methods for Characterizing Comonomer Composition in Ethylene 1-Olefin Copolymers: 3D-TREF vs. SEC-FTIR. *Polymer* **2004**, *45*, 2657–2663. [CrossRef]
7. Wharry, S.M. Randomness in Ziegler–Natta Olefin Copolymerizations as Determined by ^{13}C-NMR Spectroscopy—The Influence of Chain Heterogeneity. *Polymer* **2004**, *45*, 2985–2989. [CrossRef]
8. Ko, Y.S.; Han, T.K.; Sadatoshi, H.; Woo, S.I. Analysis of Microstructure of Ethylene–1-Hexene Copolymer Prepared over Thermally Pretreated $MgCl_2/THF/TiCl_4$ Bimetallic Catalyst. *Polym. Sci. A Polym. Chem.* **1998**, *36*, 291–300. [CrossRef]
9. Chu, K.J.; Soares, J.B.P.; Penlidis, A.; Ihm, S.K. Effect of Prepolymerization and Hydrogen Pressure on the Microstructure of Ethylene/1-Hexene Copolymers Made with $MgCl_2$-supported $TiCl_3$ Catalysts. *Eur. Polym. J.* **2000**, *36*, 3–11. [CrossRef]
10. Mulhaupt, R.; Ovenall, D.W.; Ittel, S.D. Control of Composition in Ethylene Copolymerizations Using Magnesium Chloride Supported Ziegler–Natta Catalysts. *J. Polym. Sci. A Polym. Chem.* **1988**, *26*, 2487–2500. [CrossRef]
11. Dupuy, J.; Spitz, R. Modification of Ziegler-Natta Catalysts by Cyclopentiadienyl-type Ligands: Activation of Titanium-based Catalysts. *Appl. Polym. Sci.* **1997**, *165*, 2281–2288. [CrossRef]
12. Kang, K.K.; Oh, J.K.; Jeong, Y.T.; Shiono, T.; Ikeda, T. Highly Active $MgCl_2$-supported $CpMCl_3$ (M = Ti, Zr) Catalysts for Ethylene Polymerization. *Macromol. Rapid Commun.* **1999**, *20*, 308–311. [CrossRef]
13. Yuan, K.; Yi, J.J.; Dou, X.L.; Liu, W.J.; Huang, Q.G.; Gao, K.J.; Yang, W.T. With Different Structure Ligands Heterogeneous Ziegler–Natta Catalysts for the Preparation of Copolymer of Ethylene and 1-Octene with High Comonomer Incorporation. *Polymer* **2010**, *51*, 3859–3866.

14. Lou, J.Q.; Liu, X.Y.; Fu, Z.S.; Wang, Q.; Xu, J.T.; Fan, Z.Q. Ethylene/1-hexene copolymerization with a diisopropylphenol modified supported Ziegler–Natta catalyst. *Acta Polym. Sin.* **2009**, *8*, 748–755. [CrossRef]
15. Xia, S.J.; Fu, Z.S.; Huang, B.; Xu, J.T.; Fan, Z.Q. Ethylene/1-hexene copolymerization with $MgCl_2$-supported Ziegler–Natta catalysts containing aryloxy ligands. Part I: Catalysts prepared by immobilizing $TiCl_3$(OAr) onto $MgCl_2$ in batch reaction. *J. Mol. Catal. A Chem.* **2012**, *355*, 161–167. [CrossRef]
16. Yang, H.R.; Huang, B.; Fu, Z.S.; Fan, Z.Q. Ethylene/1-Hexene Copolymerization with Supported Ziegler–Natta Catalysts Prepared by Immobilizing $TiCl_3$(OAr) onto $MgCl_2$. *J. Appl. Polym. Sci.* **2015**, *132*, 41329. [CrossRef]
17. Xia, S.J.; Fu, Z.S.; Liu, X.Y.; Fan, Z.Q. Copolymerization of Ethylene and 1-Hexene with $TiCl_4/MgCl_2$ Catalysts Modified by 2,6-Diisopropylphenol. *Chin. J. Polym. Sci.* **2013**, *31*, 110–121. [CrossRef]
18. Kageyama, K.; Tamazawa, J.-I.; Aida, T. Extrusion Polymerization: Catalyzed Synthesis of Crystalline Linear Polyethylene Nanofibers Within a Mesoporous Silica. *Science* **1999**, *285*, 2113–2115. [CrossRef]
19. Weckhuysen, B.M.; Rao, R.R.; Pelgrims, J.; Schoonheydt, R.A.; Bodart, P.; Debras, G.; Collart, O.; Voort, P.V.D.; Vansant, E.F. Synthesis, Spectroscopy and Catalysis of [Cr(Acac)$_3$] Complexes Grafted onto MCM-41 Materials: Formation of Polyethylene Nanofibres within Mesoporous Crystalline Aluminosilicates. *Chem. A Eur. J.* **2000**, *6*, 2960–2970. [CrossRef]
20. Ye, Z.; Zhu, S.; Wang, W.-J.; Alsyouri, H.; Lin, Y.S. Morphological and Mechanical Properties of Nascent Polyethylene Fibers Produced via Ethylene Extrusion Polymerization with a Metallocene Catalyst Supported on MCM-41 Particles. *J. Polym. Sci. Part B Polym. Phys.* **2003**, *41*, 2433–2443. [CrossRef]
21. Dong, X.; Wang, L.; Jiang, G.; Zhao, Z.; Sun, T.; Yu, H.; Wang, W. MCM-41 and SBA-15 Supported Cp_2ZrCl_2 Catalysts for the Preparation of Nano-Polyethylene Fibres via in Situ Ethylene Extrusion Polymerization. *J. Mol. Catal. A Chem.* **2005**, *240*, 239–244.
22. Chen, S.; Guo, C.; Liu, L.; Xu, H.; Dong, J.; Hu, Y. Immobilization of a Zirconium Complex Bearing Bis(Phenoxyketimine) Ligand on MCM-41 for Ethylene Polymerization. *Polymer* **2005**, *46*, 11093–11098. [CrossRef]
23. Dong, X.; Wang, L.; Wang, W.; Yu, H.; Wang, J.; Chen, T.; Zhao, Z. Preparation of Nano-Polyethylene Fibers and Floccules Using MCM-41-Supported Metallocene Catalytic System under Atmospheric Pressure. *Eur. Polym. J.* **2005**, *41*, 797–803. [CrossRef]
24. Ghosh, S. Influence of Supported Vanadium Catalyst on Ethylene Polymerization Reactions: Influence of Vanadium Catalyst on Ethylene Polymerization. *Polym. Int.* **2008**, *57*, 262–267. [CrossRef]
25. Wang, N.; Shi, Z.-X.; Zhang, J.; Wang, L. The Influence of Modification of Mesoporous Silica with Polyethylene Via In Situ Ziegler—Natta Polymerization on PE/MCM-41 Nanocomposite. *J. Compos. Mater.* **2008**, *42*, 1151–1157. [CrossRef]
26. Xu, H.; Guo, C.-Y. Polymerization in the Confinement of Molecular Sieves: Facile Preparation of High Performance Polyethylene. *Eur. Polym. J.* **2015**, *65*, 15–32. [CrossRef]
27. Kumkaew, P.; Wu, L.; Praserthdam, P.; Wanke, S.E. Rates and product properties of polyethylene produced by copolymerization of 1-hexene and ethylene in the gas phase with (n-BuCp)$_2$$ZrCl_2$ on supports with different pore sizes. *Polymer* **2003**, *44*, 4791–4803. [CrossRef]
28. Ko, Y.S.; Woo, S.I. Shape and diffusion of the monomer-controlled copolymerization of ethylene and alpha-olefins over Cp_2ZrCl_2 confined in the nanospace of the supercage of NaY. *J. Polym. Sci. A Polym. Chem.* **2003**, *41*, 2171–2179. [CrossRef]
29. Kumkaew, P.; Wanke, S.E.; Praserthdam, P.; Danumah, C.; Kaliaguine, S. Gas-phase ethylene polymerization using zirconocene supported on mesoporous molecular sieves. *J. Appl. Polym. Sci.* **2003**, *87*, 1161–1177. [CrossRef]
30. Ko, Y.S.; Lee, J.S.; Yim, J.-H.; Jeon, J.-K.; Jung, K.Y. Influence of Nanopores of MCM-41 and SBA-15 Confining (n-BuCp)$_2$$ZrCl_2$ on Copolymerization of Ethylene-α-Olefin. *J. Nanosci. Nanotechnol.* **2010**, *10*, 180–185. [CrossRef]
31. Paredes, B.; van Grieken, R.; Carrero, A.; Suarez, I.; Soares, J.B.P. Ethylene/1-Hexene Copolymers Produced with MAO/(nBuCp)$_2$$ZrCl_2$ Supported on SBA-15 Materials with Different Pore Sizes. *Macromol. Chem. Phys.* **2011**, *212*, 1590–1599. [CrossRef]
32. Lee, J.S.; Yim, J.-H.; Jeon, J.-K.; Ko, Y.S. Polymerization of Olefins with Single-Site Catalyst Anchored on Amine-Functionalized Surface of SBA-15. *Catal. Today* **2012**, *185*, 175–182. [CrossRef]
33. Lee, J.S.; Ko, Y.S. Control of the molecular structure of ethylene-1-hexene copolymer by surface functionalization of SBA-15 with different compositions of amine groups. *J. Mol. Catal. A Chem.* **2014**, *386*, 120–125. [CrossRef]
34. Ahmadjo, S.; Arabi, H.; Zohuri, G.; Nekoomanesh, M.; Nejabat, G.; Mortazavi, S.M.M. Preparation of Ethylene/α-Olefins Copolymers Using (2-RInd)$_2$$ZrCl_2$/MCM-41 (R:Ph,H) Catalyst, Microstructural Study. *J. Therm. Anal. Calorim.* **2014**, *116*, 417–426. [CrossRef]
35. Wang, X.; Han, X.Y.; Ren, F.; Xu, R.W.; Bai, Y.X. Porous Organic Polymers-Supported Metallocene Catalysts for Ethylene/1-Hexene Copolymerization. *Catalysts* **2018**, *8*, 146. [CrossRef]
36. Semsarzadeh, M.A.; Aghili, A. Novel Preparation of Polyethylene from Nano-extrusion Polymerization Inside the Nano-channels of MCM-41/$MgCl_2$/$TiCl_4$ Catalysts. *J. Macromol. Sci. Part A* **2008**, *45*, 680–686. [CrossRef]
37. Jafariyeh-Yazdi, E.; Tavakoli, A.; Abbasi, F.; Parnian, M.J.; Heidari, A. Bi-supported Ziegler–Natta $TiCl_4$/MCM-41/$MgCl_2$ (Ethoxide Type) Catalyst Preparation and Comprehensive Investigations of Produced Polyethylene Characteristics. *J. Appl. Polym. Sci.* **2020**, *137*, 48553. [CrossRef]
38. Zhang, W.; Zhou, S.; Zhang, R. Ethylene Polymerization Catalyzed by $TiCl_4/MgCl_2$/MCM-41 Catalytic System. *Des. Monomers Polym.* **2007**, *10*, 469–475. [CrossRef]
39. Li, D.; Lei, J.; Wang, H.; Jiang, M.; Zhou, G. Nanofibrous Ultrahigh Molecular Weight Polyethylene Synthesized Using $TiCl_4$ as Catalyst Supported on MCM-41 and SBA-15. *Polym. Bull.* **2012**, *68*, 1565–1575. [CrossRef]

40. Nejabat, G.-R.; Nekoomanesh, M.; Arabi, H.; Emami, M.; Aghaei-Nieat, M. Preparation of Polyethylene Nano-Fibres Using Rod-like MCM-41/$TiCl_4$/$MgCl_2$/THF Bi-Supported Ziegler-Natta Catalytic System. *Iran. Polym. J.* **2010**, *19*, 79–87.
41. Yang, F.; Zhang, X.; Zhao, H.; Chen, B.; Huang, B.; Feng, Z. Preparation and Properties of Polyethylene/Montmorillonite Nanocomposites By in Situ Polymerization. *J. Appl. Polym. Sci.* **2003**, *89*, 3680–3684. [CrossRef]
42. Zhao, H.; Zhang, X.; Yang, F.; Chen, B.; Jin, Y.; Li, G.; Feng, Z.; Huang, B. Synthesis and Characterization of Polpropylene/Montmorillonite Nanocomposites via an in-Situ Polymerization Approach. *Chin. J. Polym. Sci.* **2003**, *21*, 413–418.
43. Di Noto, V.; Bresadola, S. New Synthesis of a Highly Active δ-$MgCl_2$ for $MgCl_2$/$TiCl_4$/$AlEt_3$ Catalytic Systems. *Macromol. Chem. Phys.* **1996**, *197*, 3827–3835. [CrossRef]
44. Soga, K. Ziegler-Natta Catalysts for Olefin Polymerizations. *Prog. Polym. Sci.* **1997**, *22*, 1503–1546. [CrossRef]
45. Chien, J.C.W.; Wu, J.C.; Kuo, C.I. Magnesium chloride supported high-mileage catalysts for olefin polymerization. V. BET, porosimetry, and X-ray diffraction studies. *J. Polym. Sci. Polym. Chem. Ed.* **1983**, *21*, 737–750. [CrossRef]
46. Nakayama, Y.; Bando, H.; Sonobe, Y.; Fujita, T. Development of single-site new olefin polymerization catalyst system using $MgCl_2$-based activators: MAO-free $MgCl_2$-supported FI catalyst systems. *Bull. Chem. Soc. Jpn.* **2004**, *77*, 617–625. [CrossRef]
47. Busico, V.; Causà, M.; Cipullo, R.; Credendino, R.; Cutillo, F.; Friederichs, N.; Lamanna, R.; Segre, A.; Castelli, V.V.A. Periodic DFT and high-resolution magic-angle-spinning (HR-MAS) ^{1}H NMR investigation of the active surfaces of $MgCl_2$-supported Ziegler-Natta catalysts, The $MgCl_2$ matrix. *J. Phys. Chem. C* **2008**, *112*, 1081–1089. [CrossRef]
48. Singh, G.; Kaur, S.; Makwana, U.; Patankar, R.B.; Gupta, V.K. Influence of internal donors on the performance and structure of $MgCl_2$ supported titanium catalysts for propylene polymerization. *Macromol. Chem. Phys.* **2009**, *210*, 69–76. [CrossRef]
49. Redzic, E.; Garoff, T.; Mardare, C.C.; List, M.; Hesser, G.; Mayrhofer, L.; Hassel, A.W.; Paulik, C. Heterogeneous Ziegler–Natta catalysts with various sizes of $MgCl_2$ crystallites: Synthesis and characterization. *Iran. Polym. J.* **2016**, *25*, 321–337. [CrossRef]
50. Akram, M.A.; Liu, X.Y.; Jiang, B.Y.; Zhang, B.; Ali, A.; Fu, Z.S.; Fan, Z.Q. Effect of alkylaluminum cocatalyst on ethylene/1-hexene copolymerization and active center distribution of $MgCl_2$-supported Ziegler-Natta catalyst. *J. Macromol. Sci. Part A* **2021**, *58*, 539–549. [CrossRef]
51. Jiang, B.Y.; Weng, Y.H.; Zhang, S.J.; Zhang, Z.; Fu, Z.S.; Fan, Z.Q. Kinetics and mechanism of ethylene polymerization with $TiCl_4$/$MgCl_2$ model catalysts: Effects of titanium content. *J. Catal.* **2018**, *360*, 57–65. [CrossRef]
52. Xu, T.; Yang, H.R.; Fu, Z.S.; Fan, Z.Q. Effects of comonomer on active center distribution of $MgCl_2$/$TiCl_4$-$AlEt_3$ catalyst in ethylene/1-hexene copolymerization. *J. Organomet. Chem.* **2015**, *798*, 328–334. [CrossRef]